

## A RESTING-STATE FUNCTIONAL MRI STUDY: ALTERATIONS OF NEURAL ACTIVITY IN PATIENTS WITH PREMATURE VENTRICULAR CONTRACTION

SHUAI GUO<sup>1</sup>, DAYANG HUANG<sup>1</sup>, DECHUN YIN<sup>1</sup>, LULU LI<sup>2</sup>, XIUFEN QU<sup>1,\*</sup>

<sup>1</sup>Department of Cardiology, The First Affiliated Hospital of Harbin Medical University, Harbin, China - <sup>2</sup>Department of Radiology, The First Affiliated Hospital of Harbin Medical University, Harbin, China

### ABSTRACT

**Background:** The brain centers play an important role in the pathophysiology of arrhythmogenesis. Resting-state functional magnetic resonance imaging (rs-fMRI) is an elegant method for assessing the brain-heart interactions.

**Methods:** This study was performed with healthy participants (CON) and premature ventricular contraction (PVC) patients. The rs-fMRI data were obtained on a Philips 3.0 Achiva scanner. We combined different methods to identify brain function.

**Results:** The PVC group showed decreased the amplitude of low-frequency fluctuations (ALFF) mainly in the right caudate nucleus and right insula, increased fractional-amplitude of low-frequency fluctuations (fALFF) mainly in the right cuneus. The regional homogeneity (ReHo) value of the PVC group were mainly decreased in the left middle temporal gyrus compared with those recorded in the CON group. The PVC group showed significantly higher seed-based functional connectivity (FC) with the right parahippocampal gyrus, right amygdala, right lingual gyrus, right inferior temporal gyrus, left caudate nucleus, left anterior cingulate, and left middle frontal gyrus. However, it showed lower FC with the right inferior frontal gyrus triangular part and right thalamus.

**Conclusion:** The patterns of spontaneous brain activity, synchronization activity, and FC in the PVC and CON groups were different. The areas with altered brain activity in patients with PVC are considered the epicenter of emotional and behavioral expression, indicated that emotion via regulation of the central nervous system may contribute to the development of ventricular arrhythmia.

**Keywords:** Resting-state fMRI, premature ventricular contraction, spontaneous brain activity, synchronization activity, functional connectivity.

DOI: 10.19193/0393-6384\_2020\_4\_397

Received November 30, 2019; Accepted January 20, 2020

### Introduction

The morbidity and mortality of cardiac arrhythmia are high in the population, presently therapies have limitations, including the insufficient knowledge of neural activity<sup>(1-7)</sup>.

There exists a complex and dynamic interaction between the heart and brain, the brain centres affect cardiac electrophysiology<sup>(8)</sup>. It is well known that brain injury can cause cardiovascular complications, but even without neurological trauma and with a structurally normal heart, the central nervous system (CNS) is a powerful modulator of cardiac excitability<sup>(9-12)</sup>, especially in the setting of negative emotions<sup>(3)</sup>, and plays an important role in the genesis of ventricular arrhythmias.

Negative emotion has an asymmetric effect on cortical activity, and there does not appear to be one arrhythmia center in the brain but rather multiple areas involved in the process. Given the important role of neural activity, understanding the relationship between abnormal neuromodulation and cardiac electrophysiology could have important treatment implications. However, most studies target on the autonomic nervous system, the understanding of the effects of CNS on cardiac electrophysiology is not well established, research on humans is limited, and mainly focus on pathology condition. Neglecting brain-related arrhythmias may lead to delayed diagnosis and inappropriate treatment<sup>(13-17)</sup>.

As such, the value of neuroscience-based cardiovascular research is increasingly evident.

Central neural activity influences cardiac electrophysiology are coming to light in the new era of functional neuroimaging<sup>(18, 19)</sup>. Functional MRI is a very potential technology to assess the heart-brain interaction, especially in response to emotion changes<sup>(18)</sup>, has been widely used in studies of neurologic, neurosurgical, and psychiatric disorders. However, it is rarely used in research related to the cardiovascular system<sup>(4, 10)</sup>.

In our study, we used the rs-fMRI technique to construct a bridge between the brain and heart in humans. We collected rs-fMRI data to compare the differences in rs-BOLD signal between healthy participants and patients with premature ventricular contraction. We sought to determine whether alterations of spontaneous brain activity, synchronization activity, and functional connectivity exist in patients with arrhythmia, provide new insights into future novel therapies to prevent ventricular arrhythmia.

## Materials and methods

### Participants

Our study was approved by The Ethics Committee of The First Affiliated Hospital of Harbin Medical University, consisted of a control group (CON) and a premature ventricular contraction group (PVC). The PVC is defined as that patients with a PVC burden >10% but <30%, based on 24 hour Holter recording.

#### The exclusion criteria:

- Patients with structural heart disease;
- History of psychiatric/neurological disorders;
- Organic brain syndrome;
- Respiratory system diseases.

### MRI Acquisition and data preprocessing

All participants, scanned with a 3.0-T Philips Achiva 3.0T scanner.

*Sequence of gradient echo-planar image was used for the rs-fMRI scan with the following parameters:*

- Repetition time/echo time = 2,000/40 ms;
- Flip angle = 90°;
- Slice thickness = 4 mm;
- Matrix = 128×128; volumes = 200;
- And field of view = 230×230 mm<sup>2</sup>.

During the fMRI scanning, individuals presented with sinus rhythm, and were asked to keep their eyes closed, relax, limit movement, and stay awake. We used Statistical Parametric Mapping 12 (SPM12, <http://www.fil.ion.ucl.ac.uk/spm/>) to confirm the quality of rs-fMRI images. Participants with

head motion exceeded 1.5 mm or 1.5° were excluded. Data were analyzed using DPARSF (<http://rfmri.org/DPARSF>)<sup>(5)</sup>, based on SPM12 on the MATLAB 2019a platform (The MathWorks, Natick, MA, USA).

*Functional image data were preprocessed as follows:*

- Removing the first 10 time points;
- Slice timing using the 27th slice as the reference;
- Correcting head movements;
- Normalized to Montreal Neurological Institute (MNI) space using a standard MNI template, and regressing nuisance covariables, including white matter signal, cerebral spinal fluid signal, head motion and linear trends.

### ALFF, fALFF, ReHo and seed-based functional connectivity analysis

For ALFF and fALFF analysis, the time series were transformed into the frequency domain using a Fourier transform.

The square root of the power spectrum was calculated and averaged across 0.01-0.08 Hz within each voxel<sup>(20-23)</sup> to obtain raw ALFF value. Subsequently, the raw ALFF value was divided by mean ALFF value of the whole brain. The fALFF value was the ratio of the power spectrum of low frequency (0.01-0.08 Hz) to that of the entire frequency range. ReHo analysis was performed on the functional images after preprocessing, ReHo maps were produced by calculating the concordance of the Kendall coefficient of the time series of a given voxel with its 26 nearest neighbors. The generated ReHo images were smoothed using a Gaussian kernel (4-mm full-width-half-maximum) for further statistical analysis<sup>(24)</sup>. The ALFF, fALFF, and ReHo values of each individual were transformed to Z scores to enable further comparison between groups.

Seeds were derived from ALFF, fALFF and ReHo calculations. A mean time series for each seed was extracted as a reference. Subsequently, Pearson correlation coefficient (r) was applied to quantify the relationship between the seeds and the other brain regions. As a result, a correlation map was produced for each seed. The resulting r values were converted into Z values through Fisher's R-to-Z transformation (Fisher, 1915). FC results were visually presented by the BrainNet Viewer toolbox (<http://www.nitrc.org/projects/bnv/>)<sup>(20)</sup>.

### Statistical analysis

The difference of quantitative demographic data between the two groups were calculated by

two-sample t-test. Fisher’s Exact Test was used for the analysis of categorical demographic data. Group comparisons of ALFF, fALFF, ReHo, and FC results were performed using a two-sample t test using the statistics module of the DPABI toolbox (<http://rfmri.org/DPABI>)<sup>(22)</sup>, with age, sex, and head motion as covariates.

The results were corrected for multiple comparisons using the AlphaSim program (<http://afni.nih.gov/afni/docpdf/AlphaSim.pdf>). The statistical threshold for each voxel was set at  $p < 0.001$  with an extent threshold of cluster size  $> 50$  voxels, which yielded a corrected threshold of  $p < 0.01$ .

**Results and discussion**

*Patient characteristics*

This study involved 10 healthy participants and 11 patients with PVC. The PVC and CON groups did not show statistically significant differences with respect to characteristics, including age, sex, education level, and the parameters of echocardiography (Table 1).

Characteristic	PVC (n=11)	CON (n=10)	P-value
Age (years)	54.44±13.98	57.63±11.56	0.62
Sex (M:F)	7:4	5:5	0.67
LVEF (%)	67.22±5.45	64.75±6.27	0.40
LVEDd (mm)	47.78±3.77	46.63±4.17	0.56
RVEDd (mm)	19.78±1.72	20.38±3.34	0.64
LA (mm)	35±2.6	36.38±1.3	0.20
RA: long axis (mm)	44.11±2.52	41.88±3.76	0.17
RA: short axis (mm)	35.33±3.84	32.63±1.85	0.09
Education (years)	12.89±2.76	13.13±3.04	0.87

**Table 1:** Demographic and clinical characteristics in different groups.

*M, male; F, female; LVEF, left ventricular ejection fraction; LVEDd, left ventricular end diastolic diameter; RVEDd, right ventricular end diastolic diameter; LA, left atrium; RA, right atrium.*

*fALFF, ALFF, and ReHo*

Compared with the CON group, the PVC group showed decreased ALFF mainly in the right caudate nucleus and right insula (Table 2 and Figure 1A). The PVC group showed increased fALFF mainly in the right cuneus (Table 2 and Figure 1B).

The values of the PVC group were mainly decreased in the left middle temporal gyrus (ReHo) compared with those recorded in the CON group (Table 2 and Figure 1C).

		Cluster size	Brain region	Peak t-value	MNI coordinate		
					x	y	z
ALFF	PVC<CON	62	Caudate nucleus (R)	-3.95	15	18	-9
		69	Insula (R)	-5.01	33	3	12
fALFF	PVC>CON	52	Cuneus (R)	5.21	15	-75	27
ReHo	PVC<CON	110	Middle temporal gyrus (L)	-5.07	-51	-51	3

**Table 2:** Regions of change in the BOLD signal in ALFF, fALFF, and ReHo between the PVC and CON groups.

*The coordinates are shown in the Montreal Neurological Institute (MNI) standard space. Seeds were labeled for the FC analysis. BOLD, blood oxygenation level-dependent; ALFF, amplitude of low frequency fluctuation; fALFF, fractional amplitude of low frequency fluctuation; ReHo, regional homogeneity; R, right; L, left.*

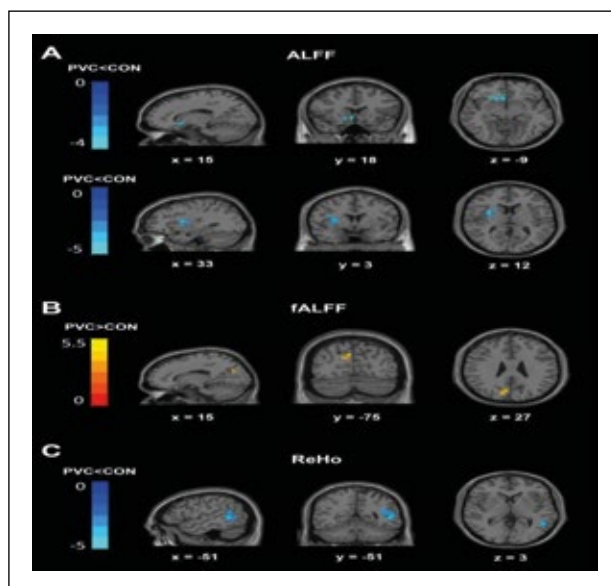


**Figure 1:** PLFF (A), fALFF (B), and ReHo (C) differences between the PVC and CON groups. (A) Decreased ALFF (blue) in the right caudate nucleus and the right insula in the PVC group compared with the CON group. (B) Increased fALFF (red) in the right cuneus in the PVC group compared with the CON group. (C) Decreased ReHo (blue) in the left middle temporal gyrus in the PVC group compared with the CON group. Color bar indicates the T score. x, y, and z denote the Montreal Neurological Institute coordinates. ALFF, amplitude of low frequency fluctuation; fALFF, fractional amplitude of low frequency fluctuation; ReHo, regional homogeneity.

*Seed-based functional connectivity*

The results of the seed-based FC analysis between the PVC and CON groups are shown in Table 3 and Figure 2. With the seed placed in right caudate nucleus, the PVC group showed significantly higher FC with the right parahippocampal gyrus, right amygdala. With the seed placed in right insula, the

PVC group showed lower FC with the right inferior frontal gyrus triangular part. Selecting the right cuneus as the seed, the PVC group showed significantly higher FC with the right lingual gyrus, but lower FC with the right thalamus. Left middle temporal gyrus-based FC analysis showed, the PVC group presented higher FC with the right inferior temporal gyrus, left caudate nucleus, left anterior cingulate, and left middle frontal gyrus.

Seed	Cluster size	Main brain region	Peak <i>t</i> -value	MNI coordinate		
				x	y	z
CAU.R	54	Parahippocampal gyrus (R) Amygdala (R)	5.3	21	0	-27
INS.R	58	Inferior frontal gyrus, triangular part (R)	-3.5	45	24	30
CUN.R	56	Lingual gyrus (R)	7.04	15	-84	-6
		Thalamus (R)	-6.08	15	-30	12
MTG.L	101	Inferior temporal gyrus (R)	5.23	45	-54	-15
		Caudate nucleus (L) Anterior cingulate (L)	5.52	-12	18	9
		Middle frontal gyrus (L)	4.5	-33	18	48

**Table 3:** Significantly altered regions in seed-based functional connectivity between the PVC and CON groups. The coordinates are shown in the Montreal Neurological Institute (MNI) standard space. R, right; L, left. CAU.R, the right caudate nucleus; INS.R, right insula-seed; CUN.R, right cuneus-seed; MTG.L, left middle temporal gyrus.

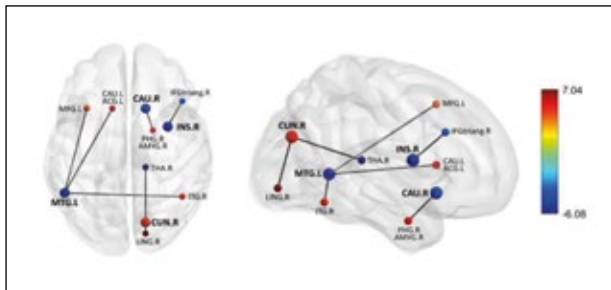


**Figure 2:** Resting-state functional connectivity maps; seeds were derived from the ALFF, fALFF, and ReHo calculations of the PVC and CON groups.

Compared with the CON group, in the right caudate nucleus-seed (CAU.R) network, increased functional connectivity in the PVC group was mainly located in the right parahippocampal gyrus (PHG.R) and right amygdala (AMYG.R). In the right insula-seed (INS.R) network, decreased functional connectivity was mainly located in the right inferior frontal gyrus triangular part (IFGtriang.R). In the right cuneus-seed (CUN.R) network, increased functional connectivity was mainly located in the right lingual gyrus (LING.R), whereas decreased

functional connectivity was mainly located in the right thalamus (THA.R). In the left middle temporal gyrus-seed (MTG.L) network, increased functional connectivity was mainly located in the right inferior temporal gyrus (ITG.R), the left caudate nucleus (CAU.L), the left anterior cingulate (ACG.L), and the left middle frontal gyrus (MFG.L). Color bar indicates the T score.

Our rs-fMRI study aimed at the correlation between brain activity and arrhythmias. ALFF and fALFF measure the power of the BOLD signal and mirror spontaneous brain activity without any underlying hypothesis. ReHo measures the synchrony of adjacent regions<sup>(15)</sup>. Seed-based functional connectivity detects abnormal functional connectivity between the seeds and the other brain regions and illustrates brain functional integration<sup>(14)</sup>. We combined these analysis methods to determine PVC related brain activity.

In the PVC group, the altered spontaneous brain activity was mainly involved limbic and right cuneus, the synchronization of regional brain activity in the left middle temporal gyrus was decreased, and the disturbed functional connectivity was mainly located in the frontal and limbic system. Our study found some areas with altered brain activity in patients with PVC, these areas are mainly associated with controlling emotional and behavioral expression. Our contribution can provide ideas and targets for further cardiac electrophysiology research. The limbic system is a complex set of structures that deal with emotions and memory, including the hippocampus, insular cortex, subcallosal gyrus, orbital frontal cortex, cingulate gyrus, parahippocampal, hypothalamus, septal nuclei, amygdala, and parts of the thalamus<sup>(2)</sup>. The right insular cortex is involved in the generation of the basic emotional states in humans<sup>(6)</sup>; emotional changes may lead to arrhythmia in patients without structural heart disease.

A previous study found that caudate had an effect on heart rate and heart rate variability under social stress and anxiety<sup>(1)</sup>. One study suggested that a hippocampal–caudate nucleus cooperation support memory performance, distinct neural representations are related to different memory systems associated with emotion and recognition.

Literatures suggest that the insula /inferior frontal gyrus is an important node in brain networks that control emotional processing. A study showed cingulate activity and fronto-temporal connectivity is associated with psychosis. A publication stated that the ability to regulate emotion promotes men-

tal well-being in health and is disrupted in psychopathologies, such as post-traumatic stress disorder. The prefrontal cortex—a region of the brain involved in executive function, behavioral coordination, and cognitive control—is particularly important in implementing the regulation of emotional response<sup>(16)</sup>.

Prefrontal and limbic circuit alterations were found in psychopathology<sup>(13)</sup>. This evidence further supports our findings; emotions contribute to ventricular arrhythmia. Combined with our analyses, the prefrontal and limbic areas of the brain are thought to be mainly responsible for PVC. Some studies found that electroacupuncture at CV4 and CV12 can modulate the limbic–prefrontal network<sup>(9)</sup>. Based on the results of our study, this treatment approach may be helpful for patients with ventricular arrhythmia.

The cuneus, a smaller lobe in the occipital lobe, is involved in basic visual processing. In addition, the volume of gray matter in the cuneus is associated with inhibitory control in patients with bipolar depression<sup>(11)</sup>.

Higher activity was found in the dorsal visual stream (including the cuneus) of pathologic gamblers<sup>(7)</sup>. Our study's results indicated that the right cuneus of the brain is a potential member of the brain network involved in the control cardiovascular function. The limitation of this study was the relatively small sample size due to strictly exclude pathologic conditions that might affect neurovascular coupling, which may decrease the robustness of the results. Comparison of before and after antiarrhythmic drug treatment should be further performed<sup>(22-33)</sup>.

## Conclusion

Our combined rs-fMRI analyses revealed a significant difference in spontaneous brain activity, synchronization activity, and functional connectivity in the PVC group. The areas of altered brain activity are mainly in the regions controlling emotional and behavioral expression.

These findings indicate that emotion via regulation of the central nervous system contribute to the development of ventricular arrhythmia, these altered brain regions may be the most promising for clinical application.

## References

- 1) Åhs, F., Sollers III, J.J., Furmark, T., Fredrikson, M., and Thayer, J.F. (2009). High-frequency heart rate variability and cortico-striatal activity in men and women with social phobia. *NeuroImage* 47(3), 815-820.
- 2) Augustine, J.R. (1996). Circuitry and functional aspects of the insular lobe in primates including humans. *Brain research reviews* 22(3), 229-244.
- 3) Buckley, U., and Shivkumar, K. (2016). Stress-induced cardiac arrhythmias: the heart-brain interaction. *Trends in cardiovascular medicine* 26(1), 78.
- 4) Chang, C., Raven, E.P., and Duyn, J.H. (2016). Brain-heart interactions: challenges and opportunities with functional magnetic resonance imaging at ultra-high field. *Philos Trans A Math Phys Eng Sci* 374(2067). doi: 10.1098/rsta.2015.0188.
- 5) Chao-Gan, Y., and Yu-Feng, Z. (2010). "DPARF: a MATLAB toolbox for "pipeline" data analysis of resting-state fMRI. *Front. Syst. Neurosci.* 4 (13), 1-7".
- 6) Craig, A.D. (2002). How do you feel? Interoception: the sense of the physiological condition of the body. *Nature reviews neuroscience* 3(8), 655.
- 7) Crockford, D.N., Goodyear, B., Edwards, J., Quickfall, J., and el-Guebaly, N. (2005). Cue-induced brain activity in pathological gamblers. *Biological psychiatry* 58(10), 787-795.
- 8) Davis, A.M., and Natelson, B.H. (1993). Brain-heart interactions. The neurocardiology of arrhythmia and sudden cardiac death. *Texas Heart Institute Journal* 20(3), 158.
- 9) Fang, J., Wang, X., Liu, H., Wang, Y., Zhou, K., Hong, Y., et al. (2012). The limbic-prefrontal network modulated by electroacupuncture at CV4 and CV12. *Evidence-Based Complementary and Alternative Medicine* 2012.
- 10) Gray, M.A., Beacher, F.D., Minati, L., Nagai, Y., Kemp, A.H., Harrison, N.A., et al. (2012). Emotional appraisal is influenced by cardiac afferent information. *Emotion* 12(1), 180-191. doi: 10.1037/a0025083.
- 11) Haldane, M., Cunningham, G., Androustos, C., and Frangou, S. (2008). Structural brain correlates of response inhibition in Bipolar Disorder I. *Journal of Psychopharmacology* 22(2), 138-143.
- 12) Herring, N., Kalla, M., and Paterson, D.J. (2019). The autonomic nervous system and cardiac arrhythmias: current concepts and emerging therapies. *Nature Reviews Cardiology*, 1-20.
- 13) Kalin, N.H. (2019). "Prefrontal Cortical and Limbic Circuit Alterations in Psychopathology". *Am Psychiatric Assoc.*
- 14) Lei, X., Zhong, M., Liu, Y., Jin, X., Zhou, Q., Xi, C., et al. (2017). A resting-state fMRI study in borderline personality disorder combining amplitude of low frequency fluctuation, regional homogeneity and seed based functional connectivity. *J Affect Disord* 218, 299-305. doi: 10.1016/j.jad.2017.04.067.
- 15) Lv, H., Wang, Z., Tong, E., Williams, L.M., Zaharchuk, G., Zeineh, M., et al. (2018). Resting-state functional MRI: everything that nonexperts have always wanted to know. *American Journal of Neuroradiology* 39(8), 1390-1399.

- 16) MacNamara, A., and K.L. Phan (2016). "Prefrontal-Limbic Brain Circuitry and the Regulation of Emotion," in *Neurobiology of PTSD: From Brain to Mind*, eds. I. Liberzon & K. Ressler. Oxford University Press), 169-196.
- 17) Natelson, B.H. (1986). Need for an integrative approach in medical diagnosis. *The American journal of medicine* 80(6), 1017.
- 18) Shivkumar, K., Ajjola, O.A., Anand, I., Armour, J.A., Chen, P.S., Esler, M., et al. (2016). Clinical neurocardiology defining the value of neuroscience-based cardiovascular therapeutics. *J Physiol* 594(14), 3911-3954. doi: 10.1113/JP271870.
- 19) Taggart, P., Critchley, H., and Lambiase, P. (2011). Heart-brain interactions in cardiac arrhythmia. *Heart* 97(9), 698-708.
- 20) Wager, T.D., Waugh, C.E., Lindquist, M., Noll, D.C., Fredrickson, B.L., and Taylor, S.F. (2009). Brain mediators of cardiovascular responses to social threat: part I: reciprocal dorsal and ventral sub-regions of the medial prefrontal cortex and heart-rate reactivity. *Neuroimage* 47(3), 821-835.
- 21) Xia, M., Wang, J., and He, Y. (2013). BrainNet Viewer: a network visualization tool for human brain connectomics. *PloS one* 8(7), e68910.
- 22) Yan, C.-G., Wang, X.-D., Zuo, X.-N., and Zang, Y.-F. (2016). DPABI: data processing & analysis for (resting-state) brain imaging. *Neuroinformatics* 14(3), 339-351.
- 23) Yang, H., Long, X.Y., Yang, Y., Yan, H., Zhu, C.Z., Zhou, X.P., et al. (2007). Amplitude of low frequency fluctuation within visual areas revealed by resting-state functional MRI. *Neuroimage* 36(1), 144-152. doi: 10.1016/j.neuroimage.2007.01.054.
- 24) Zang, Y., Jiang, T., Lu, Y., He, Y., and Tian, L. (2004). Regional homogeneity approach to fMRI data analysis. *Neuroimage* 22(1), 394-400. doi: 10.1016/j.neuroimage.2003.12.030.
- 25) Wang H, An XQ, Zhang ZY, Effect of Advanced Treatment on Ammonia Nitrogen Contained in Secondary Effluent from Wastewater Treatment Plant. *Fresenius Environ Bull* 2018; 27(4): 2043-2050.
- 26) Yang F, Yang F, Wang GY, Kong T, Wang H, Zhang CS, Effects of water temperature on tissue depletion of florfenicol and its metabolite florfenicol amine in crucian carp (*Carassius auratus gibelio*) following multiple oral doses. *Aquaculture* 2020; 515: 734542-734550.
- 27) Zhang L, Chen JH, Lei Z, He HB, Wang YS, Li YH, Preparation of soybean oil factory sludge catalyst and its application in selective catalytic oxidation denitration process. *J Clean Prod* 2019; 225: 220-226.
- 28) Zhang L, Jia Y, Zhang L, He HB, Yang C, Luo M, Miao LT, Preparation of soybean oil factory sludge catalyst by plasma and the kinetics of selective catalytic oxidation denitrification reaction. *J Clean Prod* 2019; 217: 317-323.
- 29) Zhu BZ, Pang RZ, Chevallier J, Wei YM, Vo DT, Including intangible costs into the cost-of-illness approach: a method refinement illustrated based on the PM2.5 economic burden in China. *Eur J Health Econ* 2019; 20(4): 501-511.
- 30) Chen HX, Chen YT, Liu Y, Intelligent early structural health prognosis with nonlinear system identification for RFID signal analysis. *Comput Commun* 2020; 175(1): 150-161.
- 31) Xiong Q, Zhang X, Wang W, Gu Y, A Parallel Algorithm Framework for Feature Extraction of EEG Signals on MPI. *Comput Math Method Med* 2020; 1: 1-10.
- 32) Chen H, Zhang G, Fan D, Fang L, Huang L, Nonlinear Lamb wave analysis for microdefect identification in mechanical structural health assessment. *Measurement* 2020; 164: 108026-108036.
- 33) Yang M, Abdalrahman H, Sonia U, Mohammed A, Vestine U, Wang M, Ebadi AG, Toughani M. The application of DNA molecular markers in the study of Codonopsis species genetic variation, a review. *Cell Mol Biol* 2020; 2: 23-30.

*Acknowledgement:*

*We thank the cardiologists in The First Affiliated Hospital of Harbin Medical University for their support.*

*Corresponding Author:*

XIUFEN QU  
Email: xiufenqu@outlook.com  
(China)